Interface Structures of III–V Semiconductor Heterostructures

SEONG-GON KIM,[1] SUNGHO KIM,[1] JUN SHEN,[1] B. Z. NOSHO,[2] S. C. ERWIN,[3] L. J. WHITMAN[3]

[1]*Department of Physics and Astronomy, Mississippi State University, Mississippi State, MS 39762*
[2]*HRL Laboratories LLC, 3011 Malibu Canyon Rd., Malibu, CA 90265*
[3]*Naval Research Laboratory, Washington, DC 20375*

Received 12 March 2003; accepted 24 April 2003

DOI 10.1002/qua.10687

ABSTRACT: We report first-principles calculations of the electronic and geometric structure of the (110) cross-sectional surfaces on InAs/GaSb superlattices and compare the results to scanning tunneling microscopy images of filled electronic states. We also study the atomic scale structure of (001) interface surfaces and the adsorption of deposited atoms on these surfaces to simulate the process occurring during the heterostructure growth. In both the predicted and measured images the InAs (110) surfaces appear lower than GaSb, a height difference we show is caused primarily by differences in the electronic structure of the two materials. In contrast, local variations in the apparent height of (110) surface atoms at InSb- or GaAs-like interfaces arise primarily from geometric distortions associated with local differences in bond length. We further observed that both Ga- and Sb-terminating (001) surfaces showed dimerization of surface atoms. Ga-terminating (001) surfaces exhibited substantial buckling of surface atoms while Sb-terminating (001) surfaces did not show appreciable buckling. The adsorption of arsenic atoms occurred preferably at the bridge sites between the dimerized Sb atoms on Sb-terminating (001) surfaces. Indium atoms, on the other hand, were observed to have somewhat equal probabilities to be adsorbed at a few different sites on Ga-terminating (001) surfaces. Our calculated energies for atomic intermixing indicate that anion exchanges are exothermic for As atoms on Ga-terminating (001) interfaces but endothermic for In atoms on Sb-terminating (001) interfaces. This difference may explain why GaAs interfaces are typically more disordered than InSb interfaces in these heterostructures.
Int J Quantum Chem 95: 561–571, 2003

Key words: gallium antimonide; interface; surface reconstruction; adsorption; heterostructures

Correspondence to: S.-G. Kim; e-mail: kimsg@erc.msstate.edu

Introduction

The surface reconstruction and adsorption of atoms on reconstructed surfaces play pivotal roles in understanding the epitaxial growth of semiconducting materials [1–3]. The III–V semiconductors have a zinc-blende crystal structure made of group-III atoms and group-V atoms. One particular family of III–V semiconductors—namely, InAs, GaSb, AlSb, and their related alloys—is called "6.1 Å" semiconductors because they all have lattice parameters close to this value. When thin layers of different III–V semiconductors are grown in an alternating fashion using techniques such as molecular beam epitaxy (MBE), the materials scientists classify them as III–V semiconductor heterostructures. Because of their near-match lattice parameters and the same crystal structure, materials scientists can combine different sets of III–V semiconductors to produce materials with a variety of band alignments. The 6.1 Å family of semiconductors are combined to heterostructures to fabricate a variety of technologically important devices such as field effect transistors [4], resonant tunneling structures [5, 6], infrared lasers [7], and infrared detectors [8].

Cross-sectional scanning tunneling microscopy (XSTM) has emerged as a powerful technique to characterize III–V semiconductor heterostructures [2, 9–18]. Precise characterization of these materials is made possible by the fact that a zinc-blende III–V crystal readily cleaves along the {110} faces, producing a nearly defect-free surface that presents a cross-sectional view through a single lattice plane of structures grown on (001) substrates [9]. Tunneling microscopy is in particular useful for III–V (110) surfaces because of the simple surface structure, illustrated below in Figure 5(a). The III atoms relax toward the surface and V atoms away, shifting charge between the atoms and leaving the III dangling bond essentially empty and the V surface orbital filled. Because the STM surface topography in constant-current images approximately corresponds to contours of constant integrated charge density, only the III dangling bonds are seen in empty-state images of III–V {110} surfaces, while V orbitals are seen in filled-state images [19, 20]. Therefore, XSTM images provide an apparently straightforward chemical identification of the atoms observed.

Since the first report of atom-selective STM images of GaAs (110) [19], and the observation of a heterostructure using XSTM [9], a major issue has been delineating between electronic and geometric sources of height contrast. For nominally homogeneous materials where isolated impurity atoms are observed, such as dopants or substitutional defects, electronic origins of contrast have dominated the discussions [21]. For heterostructures, there are three contrast issues to be considered. First, the different III–V materials in a heterostructure usually have a different topographic height in filled-state images. Until the past few years [2, 14–17], discussion of this difference focused on electronic effects, specifically on the band gaps and band alignments (for filled states, the valence band maximum) and the associated number of bands contributing to the tunneling [9–13]. The second contrast issue is related to the relative appearance of point defects associated with interdiffusion between the materials. For example, Harper et al. originally described As defects in GaSb as appearing lower in height because of the position of the As HOMO [13]. Finally, there is the local height of interfacial bonds to consider. For systems without a common anion, such as InAs/GaSb, two different types of interfacial bonds are possible (InSb and GaAs bonds in this case), and it has recently been proposed, based on crystallographic arguments, that the local XSTM height is primarily determined by local bond lengths [2, 15].

It is a well-documented fact that the compositional and structural variations at the interfaces can dramatically affect the transport and optical properties of semiconducting heterostructures [22–24]. The atomic-scale understanding of the formation of interfaces in III–V heterostructures, such as GaSb/InAs, is critically important for the advancement of microelectronic device technology. This knowledge will allow us to control the composition of interfacial bond types and reduce defects at the interface. The adsorption of As and In atoms on the surfaces of GaSb semiconductor is relevant to the initial stage of molecular beam epitaxy (MBE) growth of an InAs film on a GaSb substrate. The full understanding of adsorption process, in turn, cannot be obtained without extensive knowledge of the structure of the surfaces where these adsorption processes take place.

In this work we use first-principles methods to describe the electronic and geometric structure of the (110) surfaces of InAs/GaSb superlattices. We find that the apparent surface height difference between the two materials is primarily an electronic structure effect, but the local height differences ob-

served for InSb and GaAs interfacial bonds are mostly geometric in nature. In addition, the calculations reveal that atomic intermixing lowers the energy of GaAs interfaces, favoring disorder. We also study the atomic-scale structures that determine the reconstruction of the (001) surfaces of GaSb semiconductors and the adsorption of In and As atoms on these surfaces. Surface reconstruction on two different types of (001) surfaces, namely, Ga- and Sb-terminating surfaces, are considered. We observed that both surfaces showed strong dimerization of surface atoms. Ga-terminating surfaces exhibited substantial buckling of surface atoms, while Sb-terminating surfaces did not show any appreciable buckling. Our calculations showed that arsenic atoms would be preferably adsorbed at the bridge site between the dimerized Sb atoms on Sb-terminating surfaces. On Ga-terminating surfaces, on the other hand, In atoms were observed to have more or less equal probabilities to be adsorbed at several different sites. Our calculated energies for atomic interdifussion indicate that anion exchanges are exothermic for As atoms on Ga-terminating (001) interfaces but endothermic for In atoms on Sb-terminating (001) interfaces. This difference is consistent with the experimental observation that GaAs interfaces are typically more disordered than InSb interfaces in III–V heterostructures.

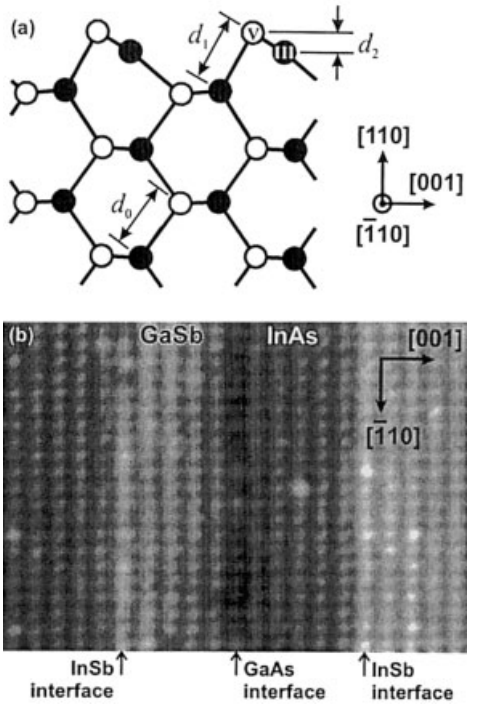

FIGURE 1. (a) Relaxed geometry of a III–V (110) surface. d_0 denotes the bond length in the bulk, d_1 the out-of-plane III–V bond length indicated, and d_2 the height difference between III and V surface atoms. (b) Constant-current, filled-state XSTM image of an InAs/GaAs superlattice.

Experimental Method

The XSTM measurements were performed in ultrahigh vacuum using InAs/GaSb superlattice samples grown by solid-source molecular beam epitaxy, as described in detail previously [2]. All images presented here are of (110) surfaces recorded with filled states at constant current (2.2–2.5 V, 150–200 pA). Figure 1(b) shows a typical filled-state XSTM image for a (110) surface. In our theoretical work, we focus on three aspects of this representative image. First, the large-scale topography shows an alternating pattern of brighter and darker bands (higher and lower apparent heights) corresponding to GaSb and InAs layers, respectively. Second, a higher Sb row is evident at InSb interfaces in this figure, whereas a lower As row is evident at the GaAs interface. Third, the degree of atomic disorder at the two interfaces is qualitatively different: InSb interfaces typically appear atomically abrupt, in contrast to GaAs interfaces, which often exhibit significant disorder.

Computational Method and Details

Our calculations are based on the first principles density functional theory (DFT) [25, 26], using ultrasoft pseudopotentials as implemented in the VASP code [27–29]. Exchange correlation effects were treated within the local density approximation (LDA) as parameterized by Ceperly and Alder [30]. The wave function of electrons are expanded in terms of plane-wave basis set [31], and all plane waves that have kinetic energy less than 150 eV are included in expanding the wave functions. The structure optimizations were performed until the energy difference between successive steps becomes less than 10^{-4} eV.

Cross-Sectional STM Calculations

Our sampling of the Brillouin zone for cross-sectional STM calculations was equivalent to using 64 k-points in the full zone of the primitive fcc cell.

We used supercell geometries to represent the InAs/GaSb heterostructures. Because of the importance of interfacial strain in this material system, we constructed supercells with starting geometries that minimized, as much as possible, any artificial strain at the interfaces. Our procedure consisted of the following three steps:

1. Bulk calculations were performed to obtain the optimized lattice parameters for four different types of zinc-blende III–V semiconductor crystals: InAs, GaSb, InSb, and GaAs.
2. For each of these four different homogeneous materials, we constructed slab supercells representing the unreconstructed (110) surfaces. This was done by periodically replicating the unit cells obtained in the previous step four times along the (110) direction, resulting in slabs containing eight atomic layers. We separated adjacent slabs by a vacuum region corresponding to five atomic layers, which we confirmed was sufficient to make the interaction between slabs negligible. All of the atoms within each slab were then relaxed within the constraint of the fixed in-plane lattice constant determined from the previous step.
3. Next, we periodically replicated the relaxed slabs six times along the (001) direction, and joined two such extended slabs together to form various III–V heterostructures with (001) interfaces and exposed (110) surfaces. For each interfacial bond case (InSb and GaAs), the two slabs were joined at a distance chosen as to allow every interfacial bond to have a bond length corresponding to the bulk lattice constant computed in step 1. The resulting supercells each contained a total of 96 atoms, with four different atomic species, corresponding to a (001) superlattice period of 24 atomic layers. Finally, the positions of all atoms were completely relaxed within the constraints of fixed superlattice period and fixed lattice constant along $[1\bar{1}0]$.

The equilibrium lattice constants calculated in step 1 are listed, along with their experimental values, in the first two columns of Table I. The agreement is good, with all errors less than 1%. The relaxed (110) surfaces of the four homogeneous materials, as obtained from step 2, show the surface buckling obtained in many previous studies [20]. The calculated buckling, illustrated in Figure 1(a) and tabulated in the last three columns of the table, is in good quantitative agreement with experiment; in particular, the height difference between III and V atoms for InAs is 0.77 Å, in excellent agreement with the value of 0.78 Å determined by low-energy electron diffraction [32].

TABLE I

Lattice constants, a_0, and bond lengths, d_i, of the relevant III–V material (Å).

	a_0[a]	a_0[b]	d_0	d_1	d_2
InAs	6.01	6.06	2.60	2.62	0.77
GaSb	6.04	6.10	2.62	2.65	0.76
InSb	6.43	6.47	2.78	2.80	0.86
GaAs	5.60	5.65	2.42	2.44	0.70

See Figure 1(a) for definitions of the different bond lengths.
[a] Lattice constant from this work.
[b] Experimental lattice constant.

After relaxing the various III–V heterostructures described in step 3, we simulated XSTM images using the method of Tersoff and Hamann [33]. To simulate filled-state images, we integrated the local density of states (LDOS) from 1 eV below the Fermi level up to the Fermi level; the surface of constant integrated LDOS then corresponds to the ideal STM topography.

Our results for InAs/GaSb heterostructures with InSb interfacial bonds are shown in Figure 2. The geometry of the fully relaxed (110) surface is displayed in Figure 2(b). As in the case of homogeneous structures, the surface atoms buckle, causing the group-V atoms (As and Sb) to move outward and the group-III atoms (In and Ga) to move inward. At the interface, Sb atoms relax still further outward so as to partially relieve compressive strain in the InSb bonds. The resulting simulated XSTM image closely resembles the measured image, as indicated by the inset of Figure 2(a) and the calculated XSTM profile across the row maxima shown in Figure 2(c). Away from the interface, the topographic maxima (from the integrated LDOS) are 0.15 Å higher on the GaSb than on the InAs, in good agreement with the height difference of about 0.2 Å typically observed in XSTM images. Interestingly, the difference in height between the actual Sb and As atoms associated with the topography is much smaller, 0.06 Å, demonstrating that the XSTM height difference is primarily caused by the surface electronic structure. Based on the calculated structure, the opposite appears true for the local topographic height difference observed at the InSb in-

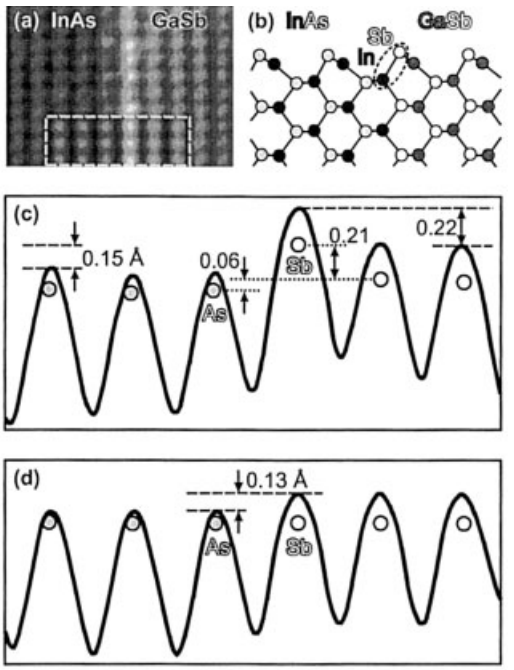

FIGURE 2. (a) XSTM image of an InAs–GaSb interface with InSb interfacial bonds. Inset: Simulated XSTM image of this structure. Both gray scales span about 1 Å. (b) Side view of the fully relaxed surface geometry for this interface. (c) Line profile for the simulated image along the [001] direction (across the row maxima). Circles denote the relaxed positions of the surface As and Sb atoms. (d) Line profile for a simulated image of two homogeneous structures joined together at their ideal lattice positions and allowed to relax the electronic but not the geometric structure.

terface. The Sb row forming InSb bonds is geometrically higher by about 0.2 Å than the Sb atoms on the GaSb surface, essentially the same height difference that occurs in the integrated LDOS, demonstrating that the observed height difference in this case is associated with the geometric structure.

To more explicitly delineate the relative contributions of geometric and electronic structure relaxation on the apparent STM topography, we calculated the electronically relaxed structure of an "ideal" InAs/GaSb heterostructure, with all interfacial atoms frozen at ideal positions. In this ideal geometry all atoms in the top layer have exactly the same height, and thus differences in heights across the computed topography originate from purely electronic effects. As shown in Figure 2(d), the electronic structure alone creates a difference in height of 0.13 Å between the InAs and GaSb surfaces, close to the 0.15-Å difference calculated with full relaxation, further supporting our conclusion that electronic structure underlies the measured height difference between the two materials.

Our analogous results for InAs/GaSb heterostructures with GaAs interfacial bonds are summarized in Figure 3, with the calculated topography again in qualitatively good agreement with that observed experimentally. At this interface the structural relaxation is different from the InSb case. As shown in Table I, GaAs bonds have the shortest surface bond length, d_1, and thus As atoms near the interface relax even further inward than Sb relaxes outward at InSb interfaces. The resulting geometric height of the As row at the GaAs interface is 0.24 Å lower than the As atoms far from the interface. However, as we saw at the InSb interface, the computed topographic height difference is almost identical, 0.23 Å, indicating that the local depression of the GaAs interface is almost completely geometric in origin.

Finally, we address why interfacial roughness appears to depend on the interfacial bond type, with GaAs interfaces in general observed to be more disordered. Experimentally, most defects occur close to the interfaces, suggesting that they arise from simple Ga–In or As–Sb exchanges across the interface, rather than from bulk defects such as vacancies or cation–anion antisites. An example of an apparent Sb atom observed in an As site at a GaAs interface is highlighted in Figure 4(a). To confirm the structural assignment of such features, we theoretically modeled such a defect by replacing

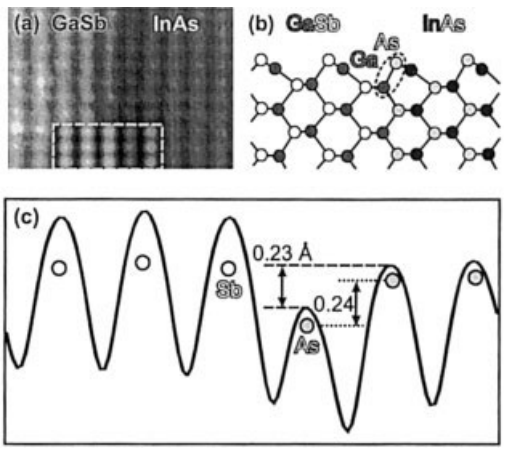

FIGURE 3. (a) XSTM image of an InAs/GaSb interface with GaAs interfacial bonds. Inset: Simulated image of this structure. (b) Side view of the fully relaxed surface geometry for this interface. (c) Line profile for the simulated image along the [001] direction.

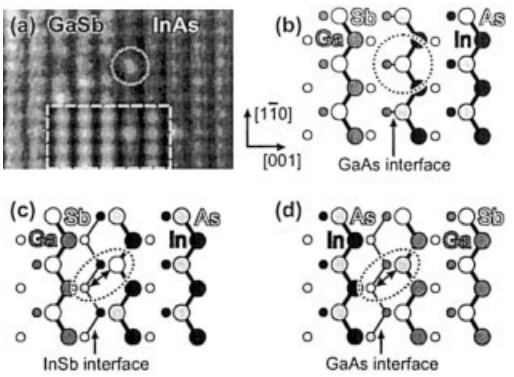

FIGURE 4. (a) XSTM image of InAs/GaSb with a GaAs interface. An apparent Sb atom in an As site at the interface is circled. Inset: Simulated XSTM image for such a defect. (b) Top view of the Sb-in-As-site defect model structure, with the top-layer atoms shown larger. (c) Model used to calculate the energetics of an As–Sb exchange across an InSb interface. (d) Model for an As–Sb exchange across a GaAs interface.

one of the surface As atoms at a GaAs interface with an Sb atom, as illustrated in Figure 4(b). The simulated XSTM image for this structure, shown in the inset of Figure 4(a), closely resembles the experimental result.

To investigate the energetics of anion interfacial defects, we consider the simplest defects that both preserve the global stoichiometry and satisfy local chemical bonding requirements, As-for-Sb exchanges. Such exchanges represent a simple mechanism for interfacial disorder at a nominally abrupt interface. We studied the energetics of exchanging adjacent As and Sb atoms both at an InSb interface and at a GaAs interface, as shown in Figures 4(c) and 4(d), respectively. The structures were fully relaxed before and after the exchange and the change in the total energy then computed. At the InSb interface, the exchange raised the total energy by 7 meV. Surprisingly, at the GaAs interface, the same process actually *lowered* the total energy by 22 meV, i.e., the formation of such defect pairs is *exothermic.* This result implies that abrupt GaAs interfaces are thermodynamically unstable. Therefore, although kinetic barriers may suppress anion exchanges, one should in general expect GaAs interfaces to be more disordered than InSb interfaces (as widely observed). This point will be further elaborated below, when we investigate the interatomic exchange diffusion during thin film growth process.

Adsorption on Interface Surfaces

Our sampling of the Brillouin zone for these calculations was equivalent to using 231 *k*-points in the full zone of the primitive fcc cell. We used supercell geometries to represent a GaSb semiconductor slab containing two different surfaces as illustrated in Figure 5. Again, the supercell was carefully prepared to have a starting geometry with minimum artificial strain. Using the optimum bulk structure obtained in the previous calculations, we first constructed slab supercells representing the unreconstructed (001) surfaces. This was done by periodically replicating the unit cell used in the GaSb bulk structure calculation along the [001] direction, resulting in slabs containing 12 atomic layers. We separated adjacent slabs by a vacuum region corresponding to 12 additional atomic layers, which we confirmed was more than sufficient to make the interaction between neighboring slabs negligible. To ensure we had enough layers of atoms across each slab, we inserted an additional pair of atomic layers of GaSb and repeated the same calculation for surface reconstruction. The added layers made no appreciable changes to all relevant physical quantities we monitored, confirming that the thickness of the slab was sufficient to reduce the interaction between the atoms on opposite sides of the same slab to a negligible level. Figure 6 shows the size of the unit cells in (001) planes. The unit cell contains enough atomic layers in lateral directions, [110] and [$\bar{1}$10], to allow up to (2 $\times$ 2) surface reconstruction. This was achieved by periodically replicating the unit cells along both [110] and [$\bar{1}$10] directions twice.

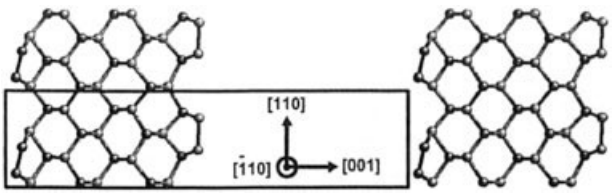

FIGURE 5. Supercell geometry containing GaSb semiconductor slab. A fully optimized structure is shown. The solid rectangular box indicates the unit cell used for the present calculations. Blue (lighter gray in gray-scale figures) spheres represent Sb atoms while black spheres represent Ga atoms.

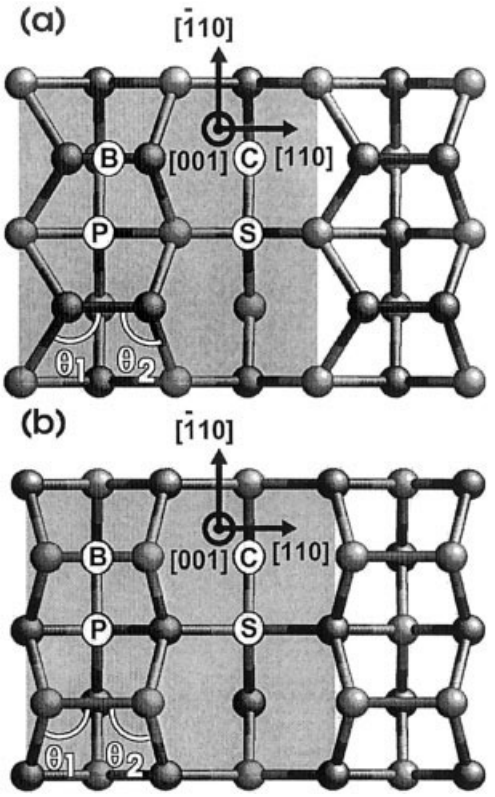

FIGURE 6. Reconstructed surfaces viewed from the top ([001] direction). (a) The Ga-terminating surface. (b) Sb-terminating surface. The shaded areas indicate the (2 × 2) unit cells used for present work. Marked positions are four of the typical adsorption sites: (B) "bridge" site, (P) "pedestal" site, (C) "cave" site, and (S) "saddle" site. See text for detailed definition of each site. There are second sets of these four adsorption sites (not marked) in the other halves of the unit cells, making a total of eight available adsorption sites. Refer to Figure 5 for the coloring scheme.

SURFACE RECONSTRUCTION

By having an even number of atomic layers in the slab, as shown in Figure 5, we were able to simulate the reconstruction of two different types of surfaces of GaSb semiconductors at the same time. We found that Ga-terminating surfaces, the left side surfaces of the slabs in Figure 5, exhibit dimerization. Figure 6(a) also shows the top view of the reconstructed but bare Ga-terminating surface. Pairs of surface Ga atoms form dimers doubling the periodicity along the [110] direction. These dimers also tend to tilt from (001) planes by about 15°, causing the surface to buckle. As a result, one of the Ga atoms was pulled in toward the plane of the underlying Sb atomic layer and formed a planar structure with two Sb atoms and the other Ga atom.

Sb-terminating surfaces, the right side surfaces of the slabs in Figure 5, also show dimerization. The top view of the Sb-terminating surface is shown in Figure 6(b). Sb dimers on Sb-terminating surfaces, however, behave differently in terms of buckling. The Sb dimers do not tilt from (001) planes and stay parallel to the surface. These behaviors can be explained by considering the average number of valence electrons associated with surface atoms and the formation of hybrid orbitals. Ga atoms are group III atoms with three valence electrons, while Sb atoms are group V atoms with five valence electrons. In bulk GaSb semiconductor, Ga and Sb atom pairs pool their valence electrons together, eight electrons for two atoms, and form sp^3 hybrid orbitals with tetrahedral coordination for zinc-blende crystal structure. Commonly, for counting purposes, Ga atoms are thought to be contributing 3/4 electron toward each bond with the Sb atom, while Sb atoms contribute 5/4 electron toward each bond with the Ga atom. Ga atoms on the surface dispense $2 * 3/4 = 3/2$ electrons to bond with Sb atoms in the inner layer. Finding no more Sb atoms to bond with, Ga atoms join together to form dimers, dispensing one additional electron per each Ga atom. Now, we have $1/2$ $(=3 - 2 * 3/4 - 1)$ electron left for each atom in Ga dimers, or one electron in total. Consequently, one of the Ga atoms forms a sp^2-like hybrid orbital (with empty p_z orbital) and gives its 1/2 electron to the other Ga atom [20, 34–37]. On the other hand, the other Ga atom forms a sp^3-like hybrid orbital and fills the last dangling bond with one remaining electron. This will create a half-filled sp^3 band and it will cause the Ga-terminating surface to be *weakly metallic* [38]. Consequently, one of the Ga atoms moves down to attain a planar three-fold coordination for itself and tetrahedral four-fold coordination for the other, preferred by sp^2-like and sp^3-like hybrid orbitals, respectively. We observed the angle θ_1 in Figure 6(a) to be 123.8°, clearly showing the two signature characteristics of the sp^2-like hybrid orbitals—planar coordination and 120° bond angles. Bond angle θ_2 in Figure 6(a) was measured to be 99.2°. Although it is distorted slightly beyond the ideal tetrahedral bond angle 109.5°, it certainly shows its preference.

Sb atoms on Sb-terminating surfaces also form dimers in a similar attempt to reduce dangling bonds. We again can count the valence electrons associated with the dimers in similar manners. Out of five of its valence electrons, Sb atoms on the

surface dispense $2 * 5/4 = 5/2$ electrons to bond with Ga atoms in the inner layer. The lack of neighbors on the surface causes Sb atoms to join together to form dimers, dispensing one additional electron per each Sb atom. Now, we have $3/2$ ($=5 - 2 * 5/4 - 1$) electron left for each atom in Sb dimers, or three electrons in total. Unlike the case of Ga dimers, one atom cannot take all three electrons into the last sp^3-like orbital. Thus, both atoms retain their electrons and fill each $3/2$ electrons into the last dangling bond of sp^3-like hybrid orbital. In other words, formation of sp^2-like hybrid orbitals is suppressed because, in that case, the remaining $3/2$ electrons must occupy p_z-like band with higher energy, and the band structure energy would be more costly. Therefore, the dimers on Sb-terminating surfaces should be parallel to (001) planes as illustrated in Figure 5. We observed the bond angles θ_1 and θ_2 in Figure 6(b) to be 102.6 and 100.0°, respectively. Wave functions for the unpaired $3/2$ electrons tend to take up more space than those of bonding electrons and cause these angles to be somewhat smaller than the ideal tetrahedral angle 109.5°.

ADSORPTION OF In_2 AND As_2 MOLECULES

In this section, we report the result of our simulations of adsorption of In_2 and As_2 molecules on the surfaces of GaSb semiconductors. We investigated both the adsorption of In and As atoms and In_2 and As_2 molecules to reproduce the experimental deposition process more closely. The added atoms are deposited initially in the form of molecules on the surfaces, but they may break up into individual atoms and settle into different adsorption sites. As mentioned previously, the ultimate purpose of these simulations is to obtain the atomic-scale understanding of the formation of interfaces in III–V heterostructures, such as GaSb/InAs. Therefore, the adsorption of In atoms was done on an Sb-terminating surface, while As atoms were adsorbed on a Ga-terminating surface. These processes simulate the formation of interfaces with two different types of bond types—InSb and GaAs. We use the optimized slab geometries obtained above as the starting configurations. These surfaces can have many different reconstructed surface structures depending on the size of the surface unit cells. Obviously, bigger periodic unit cells will produce more variety of complex adsorption patterns. In this report, however, we will consider up to (2×2) surface reconstructions only. Because we are mostly concerned with the adsorption of individual molecules, this unit cell will be adequate to capture the main effects relevant to the interface formation process during molecular beam epitaxy heterostructure crystal growth.

In Figure 6, we show the (2×2) reconstructed Ga- and Sb-terminating surfaces, respectively, viewed from the top. Four most typical lateral locations where we placed the adsorbed atoms initially are also shown. There are second sets of these four adsorption sites (not marked) in the other halves of the unit cells, making the total of eight available adsorption sites. We chose the initial height of the adsorbed atom so that the distance to the closest surface atom was the bond length between those atoms in the bulk.

Before we continue, we will define the adsorption sites as labeled in Figure 6(a). We call the site "bridge" (B) site: The As atom is placed over the midpoint of Ga dimers. The site P is called "pedestal" site: The As atom is placed between the two neighboring dimers and above Ga atom in the third top layer. The site C is the "cave" site and the added As atom is placed in the caved region, created by Ga atoms moving away due to dimerization. The site S is called "saddle" site. The Ga atom directly underneath this site has one bond bent upward and another bond bent downward in the perpendicular direction, hence the name. The adsorption sites for In atoms on Sb-terminating surface are labeled in a similar fashion as illustrated in Figure 6(a).

In both cases of bridge (B) and cave (C) sites, the As atom is placed directly above the fourth top layer consisting of Sb atoms. These sites are considered as the "proper" sites because they are the correct places for As atoms to sit if we were to grow an InAs semiconductor film on GaSb substrate with an ideal interface. In the cases of pedestal (P) and saddle (S) sites, on the other hand, As atoms are placed directly above the third top layer consisting of Ga atoms. These sites can be considered as the "wrong" sites because the As atoms on these sites have to move eventually to the "proper" sites to grow a new InAs semiconductor film with an ideal interface.

After the atoms to be adsorbed are placed at candidate sites, we relax the entire system—the slab plus the adsorbed atoms. Once the system settles down to an optimized configuration, we calculate the relative energy E_{rel} by comparing the total energy to that of the reference configuration, E_0,

$$E_{\mathrm{rel}} = E_{\mathrm{tot}} - E_0. \quad (1)$$

TABLE II

Relative energies (eV) of As_2 and In_2 molecules on Ga- and Sb-terminating surfaces, respectively.

Configuration	As_2	In_2
B+B	**0.0**[a]	0.36
B+P	0.54	0.04
B+C	2.13	0.47
B+S	1.44	0.14
P+P	5.11	**0.0**[a]
P+S	3.14	0.14
C+C	0.74	0.60
C+S	2.48	0.06
S+S	2.32	0.24
$P-z$	0.50	0.16
$C-x$	2.47	0.82
B+B exchange	**−0.55**	0.62
C+C exchange	0.03	0.29

The adsorption sites are defined in Figure 6: B, bridge; P, pedestal; C, cave; and S, saddle position. The short-hand notations *x*, *y*, and *z* are the directions the adsorbed molecules are more or less parallel and represent [110], [1$\bar{1}$0], and [001] directions, respectively. The third group with "exch" suffix represents the configurations with the interatomic exchange diffusion.

[a] Reference configurations.

We chose the configuration with lowest energy (except the ones with interatomic exchanges) to be the reference configuration for each surface we study.

Table II lists relative energies of some of the best adsorption structures for As_2 and In_2 molecules. Our calculation predicts that As atoms are most likely to be adsorbed at bridge sites on Ga-terminating surfaces. The optimized geometry of the As molecule adsorbed on Ga-terminating surface in the lowest energy configuration is shown in Figure 7. The bond length between As and Ga atom is 2.31 Å compared to its bulk value, 2.42 Å [39]. It is worth noting that the adsorption of the As atom reversed the trend of buckling: The dimers of Ga atoms are now parallel to (001) planes. Our calculation on In atom adsorption on Sb-terminating surfaces, on the other hand, predicts that there are at least three (possibly four) equally favorable configurations. B+P, B+S, P+P, and C+S configurations have virtually same relative energies for In atom adsorptions. The optimized geometry of the In atoms adsorbed in the reference configuration (P+P) on Sb-terminating surface is shown in Figure 8.

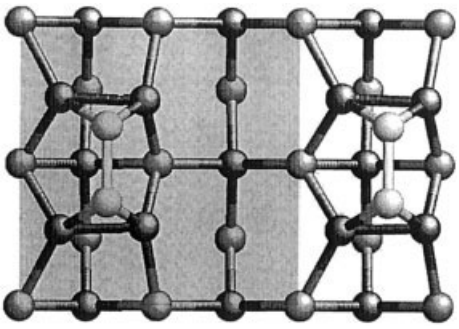

FIGURE 7. Optimized geometry of As atoms adsorbed in the B+B configuration on Ga-terminating surface. Refer to Figure 5 for the coloring scheme. White spheres represent the adsorbed As atoms.

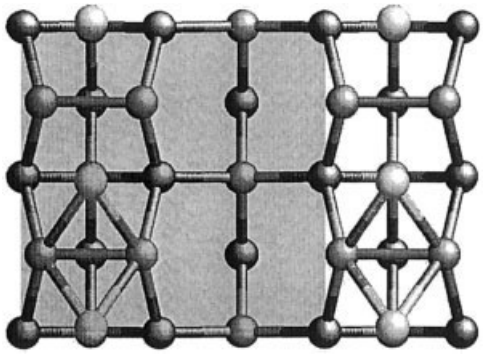

FIGURE 8. Optimized geometry of In atoms adsorbed at in the P+P configuration on Sb-terminating surface. Refer to Figure 5 for the coloring scheme. White spheres represent the adsorbed In atoms.

The bond length between In and the closest Sb atom is 2.74 Å compared to its bulk value, 2.78 Å [39]. It is a well-known fact that the atoms in molecules or on surfaces bind more tightly. Note that As molecules favor the "proper" adsorption sites (see the paragraph above for its meaning), bridge sites. Therefore, as the next As molecules come in, they will be most likely adsorbed at cave sites. As both bridge and cave sites are occupied by As atoms, the distortion due to dimerization will be completely removed and an ideal interface will be formed.

The relative energies of adsorption of In molecules on Sb-terminating surfaces seem to predict that In atoms have equal probabilities to be adsorbed in a few different configurations containing both "proper" and "wrong" sites. The relative energies of these configurations are close. Under the high-temperature condition relevant to epitaxial growth process (about 450°C), these differences would not have a significant effect. Similar to the case of As molecule adsorption on Ga-terminating surfaces, when the next In molecule joins in In

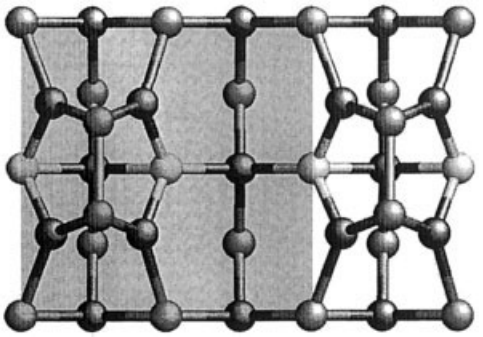

FIGURE 9. Optimized geometry of As-for-Sb interatomic diffusion on Ga-terminating surface of GaSb semiconductor. As atoms replaced Sb atoms in the second atomic layer from the top and the displaced Sb atoms are in the B+B configuration on Ga-terminating surface. Refer to Figure 5 for the coloring scheme. White spheres represent the adsorbed As atoms.

atoms are mostly likely to occupy the "proper" sites and defect-free interface will be formed in general.

INTERATOMIC EXCHANGE DIFFUSION

We also investigated the possibility of atomic intermixing during adsorption of As and In molecules. Figure 9 shows the optimized geometry of As molecules adsorbed on Ga-terminating surface and undergone through interatomic diffusion. In this case, As atoms replaced Sb atoms in the second atomic layer from the top and the displaced Sb atoms are in the B+B configuration on Ga-terminating surface. Figure 10 shows the optimized geometry of In molecules adsorbed on Ga-terminating surface and undergone interatomic diffusion process. In this case, In atoms replaced Ga atoms in the second atomic layer from the top and the displaced Ga atoms are in the C+C configuration on Sb-terminating surface. The last group of numbers in Table II summarizes our results. It is interesting to note that As-for-Sb exchange on Ga-terminating (001) surface is an exothermic process with the energy gain of more than 0.5 eV. On the contrary, In-for-Ga exchange on Sb-terminating (001) surface is an endothermic process with the energy cost of nearly 0.3 eV. This result is consistent with the result on the interatomic exchange diffusion process in the bulk environment [39]. This difference is also consistent with the experimental observation that interfaces with GaAs-type bonds are typically more disordered than interfaces with InSb-type bonds in InAs/GaSb III–V heterostructures. Further, this result provides strong evidence that the interfacial disorders are caused mainly by the interatomic diffusions occurring during the heterostructure growth process.

To give a complete and definite argument, however, a more complete study involving the kinetic effect and barrier estimation by identifying the minimum energy reaction path should be carried out. A further research along this line will provide valuable information in attaining the complete understanding of interface formation during MBE heterostructure growth.

Summary

In summary, we used first-principles electronic structure methods to clarify the interpretation of XSTM images of (110) surfaces on cleaved InAs/GaSb heterostructures, focusing on the differences between interfaces with InSb vs GaAs bonds. We find that the apparent height differences between the InAs and GaSb surfaces are largely associated with the electronic structure, whereas the local height differences at the InSb and GaAs interfaces are caused by geometric relaxation from the partial relief of local bond strain. We also investigated the atomistic process relevant to the formation of GaAs and InSb bond-type interfaces: the adsorption of In or As atoms on (001) surfaces of GaSb semiconductors. We observed that both Ga- and Sb-terminating surfaces showed dimerization of surface atoms. One of the Ga atoms of the dimers formed sp^2 hybrid orbitals while the other formed sp^3 hybrid

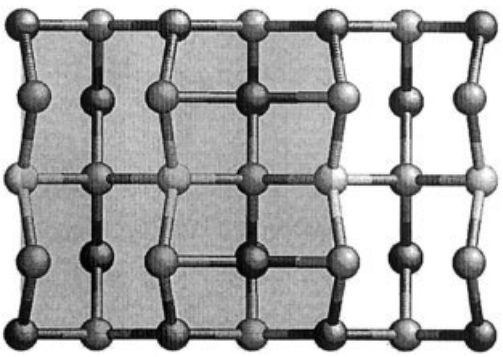

FIGURE 10. Optimized geometry of In-for-Ga interatomic diffusion on Sb-terminating surface of GaSb semiconductor. In atoms replaced Ga atoms in the second atomic layer from the top and the displaced Ga atoms are in the C+C configuration on Sb-terminating surface. Refer to Figure 5 for the coloring scheme. White spheres represent the adsorbed In atoms.

orbitals. This caused Ga dimers to tilt out of the (001) planes and the Ga-terminating surface to buckle. On the other hand, both atoms in Sb dimers formed sp^3-hybrid orbitals and consequently the Sb-terminating surfaces did not show any buckling. Our calculations also predict that arsenic atoms would be preferably adsorbed at the bridge site between the dimerized Sb atoms on Sb-terminating (001) surfaces. Indium atoms, on the other hand, were observed to have somewhat equal probabilities to be adsorbed at several different sites on Ga-terminating (001) surfaces. When an In atom was adsorbed on Ga dimers, we observed that the surface buckling was nullified and the dimers reverted back to horizontal positions. Finally, our calculations of the energies associated with interfacial exchange of anions reveal that As-for-Sb exchanges on Ga-terminating surfaces are exothermic at GaAs bond-type interfaces, but In-for-Ga exchanges on Sb-terminating surfaces are endothermic at InSb bond-type interfaces. This result is consistent with the experimental observation that GaAs bond-type interfaces are typically more disordered than InSb bond-type interfaces in the InAs/GaSb heterostructures.

ACKNOWLEDGMENTS

The authors thank B. R. Bennett and M. J. Yang for fabricating the InAs/GaSb superlattice samples. This work was supported by the Office of Naval Research and the Defense Advanced Research Projects Agency. S. G. K. acknowledges the support for this work by the Oak Ridge Associated Universities through the 2002 Ralph E. Powe Junior Faculty Award.

References

1. Barvosa-Carter, W.; Bracker, A. S.; Culbertson, J. C.; Nosho, B. Z.; Shanabrook, B. V.; Whitman, L. J.; Kim, H.; Modine, N. A.; Kaxiras, E. Phys Rev Lett 2000, 84, 4649.
2. Nosho, B. Z.; Barvosa-Carter, W.; Yang, M. J.; Bennett, B. R.; Whitman, L. J. Surf Sci 2000, 465, 361.
3. Zhang, Z.; Lagally, M. G. Science 1997, 276, 377.
4. Boos, J. B.; Kruppa, W.; Bennett, B. R.; Park, D.; Kirchoefer, S. W.; Bass, R.; Dietrich, H. B. IEEE Trans Electron Devices 1998, 45, 1869.
5. Brown, E. R.; Söderström, J. R.; Parker, C. D.; Mahoney, L. J.; Molvar, K. M.; McGill, T. C. Appl Phys Lett 1991, 58, 2291.
6. Scott, J. S.; Kaminski, J. P.; Allen, S. J.; Chow, D. H.; Lui, M.; Liu, T. Y. Surf Sci 1994, 305, 389.
7. Yang, M. J.; Moore, W. J.; Bennett, B. R.; Shanabrook, B. V. Electron Lett 1998, 34, 270.
8. Fuchs, F.; Weimer, U.; Pletschen, W.; Schmitz, J.; Ahlswede, E.; Walther, M.; Wagner, J.; Koidl, P. Appl Phys Lett 1997, 71, 3251.
9. Albrektsen, O.; Arent, D. J.; Meier, H. P.; Salemink, H. W. M. Appl Phys Lett 1990, 57, 31.
10. Gwo, S.; Chao, K.-J.; Shih, C. K.; Sadra, K.; Streetman, B. G. Phys Rev Lett 1993, 71, 1883.
11. Feenstra, R. M.; Collins, D. A.; Ting, D. Z. Y.; Wang, M. W.; McGill, T. C. Phys Rev Lett 1994, 72, 2749.
12. Smith, A. R.; Chao, K.-J.; Shih, C. K.; Shih, Y. C.; Anselm, K. A.; Streetman, B. G. J Vac Sci Tech B 1995, 13, 1824.
13. Harper, J.; Weimer, M.; Zhang, D.; Lin, C.-H.; Pei, S. S. J Vac Sci Tech B 1998, 16, 1389.
14. Feenstra, R. M. Physica B 1999, 273/274, 794.
15. Steinshnider, J.; Weimer, M.; Kaspi, R.; Turner, G. W. Phys Rev Lett 2000, 85, 2953.
16. Bruls, D. M.; Vugs, J. W. A. M.; Koenraad, P. M.; Salemink, H. W. M.; Wolter, J. H.; Hopkinson, M.; Skolnick, M. S.; Long, F.; Gill, S. P. A. Appl Phys Lett 2002, 81, 1708.
17. Zuo, S. L.; Hong, Y. G.; Yu, E. T.; Klem, J. F. J Appl Phys 2002, 92, 3761.
18. Nosho, B. Z.; Bennett, B. R.; Whitman, L. J.; Goldenberg, M. Appl Phys Lett 2002, 81, 4452.
19. Feenstra, R. M.; Stroscio, J. A. J Vac Sci Tech B 1987, 5, 923.
20. Engels, B.; Richard, P.; Schroeder, K.; Blügel, S.; Ebert, P.; Urban, K. Phys Rev B 1998, 58, 7799.
21. Ebert, P. Surf Sci Rep 1999, 33, 121.
22. Tuttle, G.; Kroemer, H.; English, J. H. J Appl Phys 1990, 67, 3032.
23. Brar, B.; Ibbetson, J.; Kroemer, H.; English, J. H. Appl Phys Lett 1994, 64, 3392.
24. Bennett, B. R.; Shanabrook, B. V.; Glaser, E. R. Appl Phys Lett 1994, 65, 598.
25. Hohenberg, P.; Kohn, W. Phys Rev 1964, 136, B864.
26. Kohn, W.; Sham, L. J. Phys Rev 1965, 140, A1133.
27. Vanderbilt, D. Phys Rev B 1990, 41, 7892.
28. Kresse, G.; Hafner, J. Phys Rev B 1993, 47, 558.
29. Kresse, G.; Furthmüller, J. Phys Rev B 1996, 54, 11169.
30. Ceperley, D. M.; Alder, B. J. Phys Rev Lett 1980, 45, 566.
31. Payne, M. C.; Teter, M. P.; Allan, D. C.; Arias, T. A.; Joannopoulos, J. D. Rev Mod Phys 1992, 64, 1045.
32. Mailhiot, C.; Duke, C. B.; Chadi, D. J. Phys Rev B 1985, 31, 2213.
33. Tersoff, J.; Hamann, D. R. Phys Rev Lett 1983, 50, 1998.
34. Lubinsky, A. R.; Duke, C. B.; Lee, B. W.; Mark, P. Phys Rev Lett 1976, 36, 1058.
35. Duke, C. B.; Lubinsky, A. R.; Lee, B. W.; Mark, P. J Vac Sci Tech 1976, 13, 761.
36. Kahn, A. Surf Sci Rep 1983, 3, 193.
37. Swarts, C. A.; McGill, T. C.; Goddard, W. A. III. Surf Sci 1981, 110, 400.
38. Whitman, L. J.; Thibado, P. M.; Erwin, S. C.; Bennett, B. R.; Shanabrook, B. V. Phys Rev Lett 1997, 79, 693.
39. Kim, S. G.; Erwin, S. C.; Nosho, B. Z.; Whitman, L. J. Phys Rev B 2003, 67, 1213066R).